Author(s): Cias, A. and Mitchell, S.C.

Title: Processing and ductile-brittle transitions in PM manganese steels

Publication year: 2005

Journal title: Powder Metallurgy Progress

ISSN: 1335-8987

Publisher: Institute of Materials Research – Slovak Academy of Sciences

Publisher's site: *http://www.sav.sk/index.php?lang=en&charset=ascii&doc=publish-journal&journal_no=18*

PROCESSING AND DUCTILE-BRITTLE TRANSITIONS IN PM MANGANESE STEELS

by

ANDRZEJ CIAS[1] and STEPHEN C MITCHELL[2]

[1]Department of Metallurgy and Materials Engineering,
Academy of Mining and Metallurgy,
Al. Mickiewicza 30,
30-059 Kraków, Poland

[2]Engineering Materials Research,
University of Bradford
Bradford, BD7 1DP.
UK

Abstract

Brittleness in manganese steels can be associated with processing in a "wet" [micro]climate resulting in the formation of continuous oxide networks. The formation of these networks can be prevented by sintering in an atmosphere, also "local" in a semi-closed container, adhering to the Ellingham-Richardson oxide reduction criteria. When this requirement is satisfied, however, further types of ductile – brittle transitions are observed. Rapid cooling, typically above 40°C/min, produces enough martensite to render Fe-(3-4)Mn-(0.6-0.7)C material macroscopically brittle. Quenched and conventionally tempered structures remain brittle. It is tentatively suggested that segregation of minor alloying/tramp element(s), as in cast materials, is responsible for this temper embrittlement. To overcome it, heat treatment at a temperature no higher than 200°C, recovery/stress relief, is recommended.

Keywords: PM processing, manganese steels, heat treatment, temper embrittlement, tramp element, ductility, oxygen segregation.

INTRODUCTION

Recently Mitchell et al [1-7] have identified the PM processing problem in Mn[-Cr] steels as oxide vein formation when the sintering atmosphere does not satisfy the Ellingham-Richardson dew point requirements. Additionally they [8] found that the necessary reducing conditions for Mn-Cr steels can be attained in flowing gases too wet for conventional processing - through the use of semi-closed containers with a supply of the volatile manganese and carbon. The mechanical properties of Fe-3%Mn-0.6%C steel sintered in semi-closed containers in dry hydrogen, technical nitrogen and mixtures thereof were comparable. They include yield and tensile strengths of ~450 and ~750 MPa, with elongation of ~ 1.8%. However, some thermal treatments, including rapid cooling from the sintering temperature, do result in embrittlement. It is the purpose of this communication to consider this occurrence and means of overcoming the problem.

EXPERIMENTAL PROCEDURES

Höganäs sponge NC100.24 was used as the base iron powder. Carbon was introduced as fine graphite (of 99.5% purity) and 3 and 4 % of manganese as Elkem low carbon ferro-manganese Fe-77%Mn- 1.3%C, milled before sieving to less than 20μm, with a median of

8µm.Starting compositions chosen were Fe-3/4Mn-0.8C. Double-cone mixing and die compaction at 660 MPa of ISO 2740, TS, dogbone and transverse rupture strength, TRS, 55x11x5mm^3 specimens were followed by sintering in nearly full semi-closed stainless steel containers with a labyrinth seal, illustrated in Fig.1. The container did not have any ferromanganese added to it [9], but was loaded to capacity, ~ 20 specimens, with any remaining space in the container being filled with ferrous ballast. It was the green compacts that were the donors of Mn and C. This arrangement provided sufficient manganese vapour to both improve the local dew point (self gettering) and minimise the loss of manganese from the compacts. The container was pushed into the hot zone of the stainless steel tube of the furnace. The furnace atmospheres were pure hydrogen or pure nitrogen with a gas flow of ~0.2 cm^{3}min^{-1} per cm^2 of furnace tube cross sectional area and an inlet dew point no worse than -60 °C. At least 20 compacts were simultaneously sintered; sintering times were 1 hour and sintering temperatures 1120 and 1250°C. There was no significant change in density from green values (~6.9g/cm^3). After sintering, the specimens were withdrawn from the hot zone to the cool zone of the furnace at 1.5 - 65°Cmin^{-1}. Some specimens cooled at a rate of 65°Cmin^{-1} were tempered at 200 - 400°C for 1 hour.

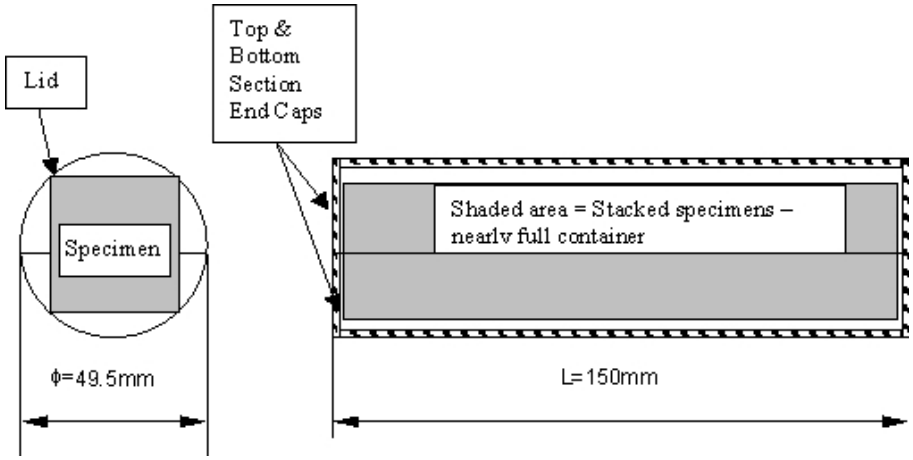

Fig. 1: Schematic of semi-closed sintering container.

Chemical analyses were performed on powders and sintered PM steels to characterise the level/uniformity of carbon, sulphur, nitrogen, oxygen, and manganese. The analytical determinations of carbon, oxygen and nitrogen were performed with Leco TC 336 and CS125 instruments. The manganese content was measured by wet chemical analysis. These properties were measured: green and sintered density, dimensional change, transverse rupture strength, impact energy, yield strength, YS, tensile strength, UTS, elongation, Young's modulus, and hardness, HV. Apparent hardness, dimensional change from green compact size and tensile properties, were determined according to ISO and MPIF Standards 43, 44 and 10, respectively. Tensile tests were conducted on a MTS 810

testing machine and transverse rupture tests on a W."Fritz Heckert" type 2010/90 machine equipped with a three point bending jig (span 28.6mm), all at a crosshead speed of 2mm/min. For metallographic investigations the samples were mounted in bakelite, polished, etched in Nital (3%HNO_3-97%methanol) and examined on a Leica DMLM optical microscope and a Zeiss Neophot2/Hanemann microhardness tester. Retained austenite was determined by X-ray diffraction.

RESULTS

Chemical analyses of Fe-3/4Mn-0.8C alloys, Tables 1 and 2, show, however, that the actual carbon contents of specimens sintered at 1120 and 1250°C were ~0.6 and ~0.5%C, respectively. The analyses further indicate that, in addition to minor Mn losses, some 0.2-0.3%, decarburisation of the steels, with concurrent oxygen losses of up to 0.1%. Only minor dimensional changes resulted from sintering; the average densities were near 7.0 g/cm^3. The higher sintering temperature resulted in more rounded porosity and slight improvement in mechanical properties. When the Fe-3Mn-0.8C alloy was cooled from the sintering temperature at rates of 10 and 40°Cmin^{-1}, even at these relatively low cooling rates, the material was observed to contain low temperature transformation products and associated residual stresses [9]. The as-sintered samples had 8.2 and 16.9% retained austenite for 12 and 30 °Cmin^{-1} cooling rates, respectively. After oil quench (cooling rate: 20-30°Cs^{-1}) this increased to 24-40 %. Thus for conventional industrial PM processing (cooling rate ~ 10°Cmin^{-1}) between 5 and 20 % retained austenite is anticipated in these Mn steels. Main microstructural features are summarised in Table 3 and Fig. 2 illustrates microstructures of Fe-3%Mn-0.8%C specimens sintered in a 100% nitrogen atmosphere at 1120 and 1250ºC, respectively.

Average mechanical properties are recorded in Tables 4 and 5 for Fe-3Mn-0.8C and in Tables 6 and 7 for the 4Mn steel. The effects of increasing Mn content and sintering temperature were to lower the tensile elongation, the reverse of the effect on the yield and tensile strengths of slowly cooled specimens. The effect of higher sintering temperature in closing residual porosity and therefore increasing the fracture strength is also apparent. Slow cooling rates favoured plasticity, which ceased to be significant at cooling rates above 30- 40ºCmin^{-1}: ductile-brittle transitions. Sintering Fe-3Mn-0.8C at 1100ºC and cooling below 30°Cmin^{-1} produced pearlite with attendant ductility (0.3-0.5%) and UTS up to 610 MPa and TRS up to 1230 MPa. At higher cooling rates, less homogeneous, macroscopically brittle microstructures, comprising pearlite, bainite, martensite and retained austenite, resulted. The best combinations of mechanical properties were attained at the lowest cooling rates. Fracture strengths of the specimens cooled at 65°Cmin^{-1} were only ~470 MPa in tension and ~1060 MPa in bending. The highest cooling rate employed in these experiments, 65°Cmin^{-1}, can be exceeded in modern industrial sinter hardening furnaces, so the results have industrial relevance.

Table 1. Results of Leco analyses of Fe-3Mn-0.8C compacts after sintering.

Sintering temperature 1120°C		
Cooling rate, °C/min	Average carbon content, %	Average oxygen content, %
1.3	0.617	0.250
55	0.550	0.187
65	0.658	0.201

Table 2. Results of Leco analyses of Fe-3Mn-0.8C compacts after sintering.

Sintering temperature 1250°C		
Cooling rate, °C/min	Average carbon content, %	Average oxygen content, %
1.4	0.496	0.130
57	0.532	0.162
65	0.530	0.151

Some of the sinter-hardened alloys (cooled at 65°Cmin^{-1}) were subsequently tempered in hydrogen at temperatures ranging from 200 to 450ºC for 1 hour (Table 8). Microstructures of specimens tempered 1 hr at 200°C (mechanical properties shown in Table 9) comprised mainly a mixture of tempered martensite, bainite and fine (divorced) pearlite (troostite), Significant improvement in properties was attained as a result of the 200ºC stress relief, e.g. 830-850MPa tensile strength with > 2% ductility for the 1250ºC sintering temperature. Results were similar for the 400ºC temper and there was an indication of temper embrittlement at ~250 ºC (Table 8), more severe for the specimens sintered at 1250 ºC. By 300ºC, Table 10, ductility, though limited, was significant. The slowly cooled specimens show similar UTS and TRS values to these of the sinter hardened, with very little retained austenite.

Table 3. Microstructure of Fe-3Mn-0.8 (nominal composition) sintered manganese steels with final carbon content.

Cooling rate, °C/min	Microstructure	
	Sintering temperature 1120°C	Sintering temperature 1250°C
1.5	Coarse lamellar pearlite	Coarse lamellar pearlite + proeutectoid ferrite
4.5 and 9	Pearlite	Pearlite + proeutectoid ferrite
18	Fine pearlite	Ultra fine pearlite + upper bainite
30	Ultra fine pearlite (troostite) + upper bainite	Lower bainite + martensite
44	Lower bainite + Martensite	Martensite + lower bainite + retained austenite
55 – 65	Lower bainite + martensite + retained austenite	Martensite + lower bainite + retained austenite

Table 4. The effect of cooling rate on the mechanical properties of Fe-3Mn-0.8C (final 0.6%C) specimens sintered at 1120ºC.

Cooling rate, °C/min	*YS*, 0.2% offset strength, MPa	Tensile strength, MPa	Tensile elongation, %	Transverse rupture strength, MPa	Cross-section hardness, HV30	Impact energy, J/cm^2
1.3	315	447	1.8	1050	169	16.5
4.8	330	478	1.0	1270	224	17.2
8.7	455	506	1.0	1230	217	10.8
15.5	450	568	0.6	1200	148	11.0
30.1	485	557	0.6	1120	172	8.2
47.0	510	559	0.5	1100	176	5.8
55.0	**brittle**	535	0.2	1000	292	5.2
60-65	**brittle**	486	0.1	1050	303	6.5

Table 5. The effect of cooling rate on the mechanical properties of Fe-3Mn-0.8C (final 0.5%C) specimens sintered at 1250ºC.

Cooling rate, °C/min	*YS*, 0.2% offset strength, MPa	Tensile strength, MPa	Tensile elongation, %	Transverse rupture strength, MPa	Cross-section hardness, HV30	Impact energy, J/cm^2
1.4	385	587	3.1	1240	166	21.3
4.7	440	595	1.7	1330	254	11.5
9.4	410	614	1.5	1310	239	9.9
20.4	325	583	1.2	1210	265	7.7
31.8	570	586	0.3	1190	282	9.4
41.1	**brittle**	521	0.2	1080	328	4.6
57.0	**brittle**	491	0.1	1090	335	4.9
60-65	**brittle**	507	0.1	990	276	4.9

Table 6. The effect of cooling rate on the mechanical properties of Fe-4Mn-0.8C (final 0.6%C) specimens sintered at 1120ºC.

Cooling rate, °C/min	0.2% offset strength, MPa	Tensile strength, MPa	Tensile elongation, %	Transverse rupture strength, MPa
4.8	422	669	1.3	1021
8.7	417	680	1.3	1116
15.5	374	651	1.2	1227
30.1	414	659	1.1	1121
47.0	**brittle**	482	0.2	1151
55.0	**brittle**	580	<0.1	1097
65	**brittle**	561	<0.1	1079

Table 7. The effect of cooling rate on the mechanical properties of Fe-4Mn-0.8C (final 0.5%C) specimens sintered at 1250ºC.

Cooling rate, °C/min	*YS*, 0.2% offset strength, MPa	Tensile strength, MPa	Tensile elongation,%	Transverse rupture strength, MPa
4.7	434	636	0.6	1467
9.4	460	600	0.4	1451
20.4	459	547	0.2	1362
31.8	**brittle**	496	<0.1	1364
41.1	**brittle**	468	<0.1	1124
57.0	**brittle**	428	<0.1	847
65	**brittle**	485	<0.1	891

Table 8. Effect of tempering on the mechanical properties of Fe-3Mn-0.8C specimens.

Sintering temp.,°C	Tempering temp., °C	*YS*, 0.2% offset strength MPa	UTS, MPa	Elonga-tion, %	TRS, MPa	Impact energy, J/cm^2
1120	None	**brittle**	470	0.1	1070	4.7
	200	410	740	1.9	1480	12.1
	250	437	700	1.0	1400	8.0
	300	430	740	1.9	1510	10.4
	350	453	700	0.9	1420	8.9
	400	460	740	1.9	1460	11.5
	450	442	677	1.7	1550	10.9
1250	None	**brittle**	460	0.1	1060	5.1
	200	470	830	2.3	1480	10.1
	250	504	790	0.9	1370	4.1
	300	470	800	1.4	1450	4.9
	350	521	840	1.0	1530	8.8
	400	500	850	2.0	1750	15.7
	450	504	704	1.2	1740	15.3

Table 9. Properties of sintered and sinter hardened Fe-3Mn-0.8C specimens sintered at 1120 and 1250ºC.

Fe-3%Mn-0.6%C convective cooling at 65ºCmin^{-1}	Sintering temperature 1120ºC	Plus stress relief 1 hr at 200ºC	Sintering temperature 1250ºC	Plus stress relief 1 hr at 200ºC
Apparent cross-section hardness, HV_{30}	305	235	310	225
TRS, MPa	1080	1470	1070	1490
0.2% offset strength, MPa	**brittle**	430	**brittle**	480
Tensile strength MPa	460	750	470	830
Tensile elongation, %	0.1	1.9	0.1	2.4
Impact energy, J/cm^2	4.9	13.0	5.2	10.5

Table 10. Average properties of 60 TRS and 54 UTS sinter- hardened Fe-3Mn-0.8C specimens tempered at 300°C for one hour.

Sintering temperature, °C	Cross-section Apparent hardness, HV30	UTS, MPa	Tensile elongation, %	TRS, MPa	Impact energy, J/cm^2
1120	227	751	2.01	1481	11.3
1250	265	827	1.82	1630	10.2

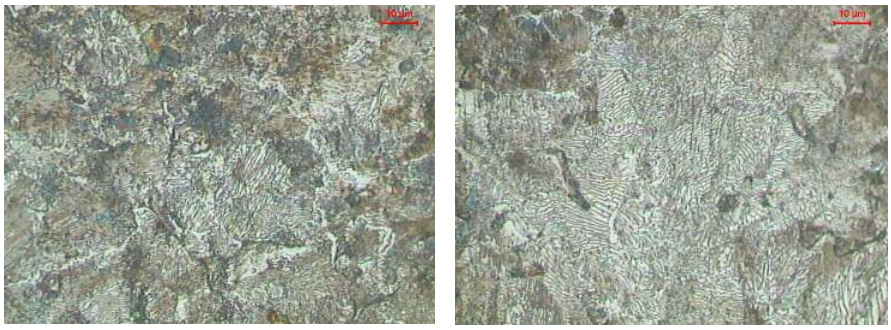

(a) (b)

Fig. 2. Scanning electron micrograph of Fe-3%Mn-0.8%C specimen sintered at (a) 1120°C and (b) 1250ºC in 100% nitrogen atmosphere.
Note larger overall grain size of the 1250ºC sintered material.

DISCUSSION AND CONCLUSIONS

The most common cause of brittleness in PM Mn steels is "incorrect" processing in atmospheres not adhering to the Ellingham-Richardson reduction criteria. This problem was overcome in the research reported above, as was the danger of oxide formation during slow cooling. This contrasts somewhat with the recent report of similar work of Dudrova et al [10] whose EDX maps of oxygen distribution showed that, although oxide networks were not generally detected after sintering at 1180°C with a dew point of -55°C, in one case oxide phase was found due to poorer processing conditions. Of numerous heat treatments of 3/4Mn-0.3C steels, this occurred for Fe-4Mn-0.3C slow-cooled, 10°Cmin^{-1}, alloy, which also exhibited brittle behaviour. The reason for this difference may lie with the use of semi -closed containers and/or a lower dew point employed in this study. The effect of reducing the partial pressure of CO in a semi-closed container is shown in Fig.3.

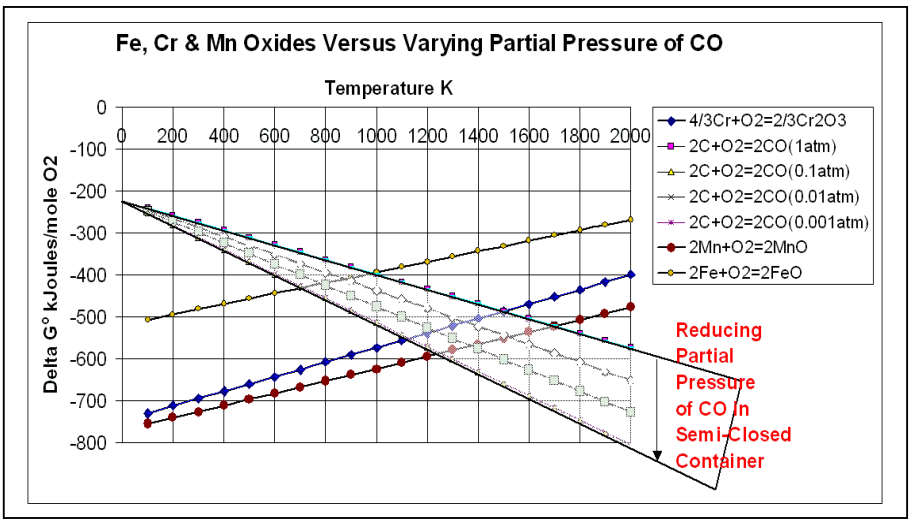

Fig . 3: Effect on reduction temperature for Fe, Cr and Mn oxides versus partial pressure of CO in a semi-closed container.

A schema of the possible reactions of sublimating manganese vapour with the flowing furnace gases (including oxygen to form manganese oxide) as a function of distance from the compact surface is shown in Salak's "Ferrous Powder Metallurgy" [11]. Accordingly the Discussion will concentrate on "clean" microstructures, martensite formation with its associated transformation stresses, their reduction /elimination and embrittlement liable to occur during tempering.

A continuous cooling transformation (CCT) diagram for the composition now studied, reproduced as Fig.4, shows upper and lower transformation regions separated by a metastable austenite bay. Typically A_{c1}=720°C and A_{c3}=782°C, whilst the martensite transformation start (M_s) temperature depends, inter alia, on the cooling rate. For industrial sintering (5-20°Cmin^{-1}) cooling curves would locate slightly to the right of curve-4 (0.5°Cs^{-1}). Thus after sintering, hardnesses around 230HV are expected, rising to around 450HV after quenching. Loss of Mn and C will raise the M_s temperature and accordingly decrease the hardness after quenching.

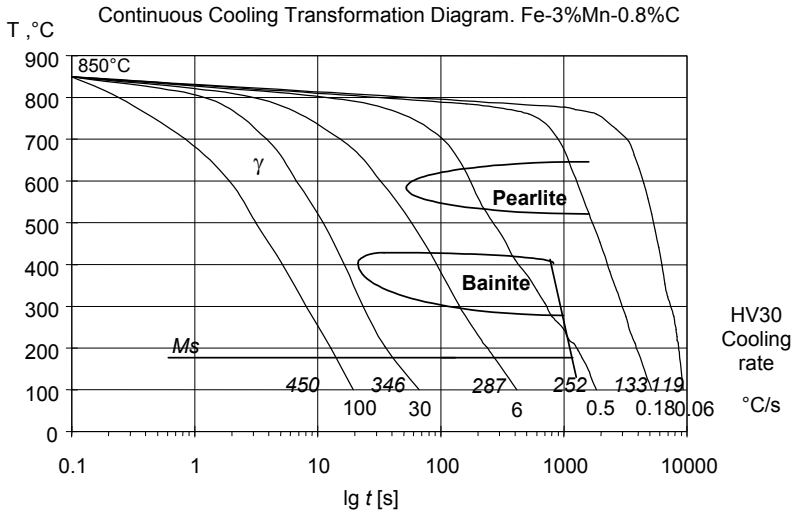

Fig.4. Continuous Cooling Transformation Diagram for Fe-3Mn-0.8C.
(Diagram plotted in collaboration with Prof. Pal Barczy - Miskolc University).

The as-sintered specimens show low impact resistance but tempering at 200°C transforms strained body-centred tetragonal martensite to a hexagonal close-packed transition carbide, ε-carbide, plus low-carbon martensite, which lowers internal stresses. It can be seen from Tables 3, 4, 5, 6 and 7 that, despite the 1250°C material being lower in final carbon, it exhibits higher hardenability. The lower C content of the 1250°C material raises M_s and M_f temperatures, which reduces the amount of retained austenite, but increases the martensite fraction. Calculated M_s and M_f temperatures are 235°C and 38°C for the 1250°C sintered material and 205°C and 8°C for the 1120°C sintered material. The 1250°C sintered material has greater austenite grain size compared with the 1120°C material, which decreases grain boundary area. This decrease reduces the sites available for the nucleation of ferrite and pearlite, with the result that these transformations are retarded, and hardenability is therefore increased. ASTM grain size versus hardenability tables suggest, please see Fig. 5, an increase from G5 to G3, i.e. 50 to ~100 microns intercept measurement, will ensure that a 0.5% C material has higher hardenability than a 0.6% C material.

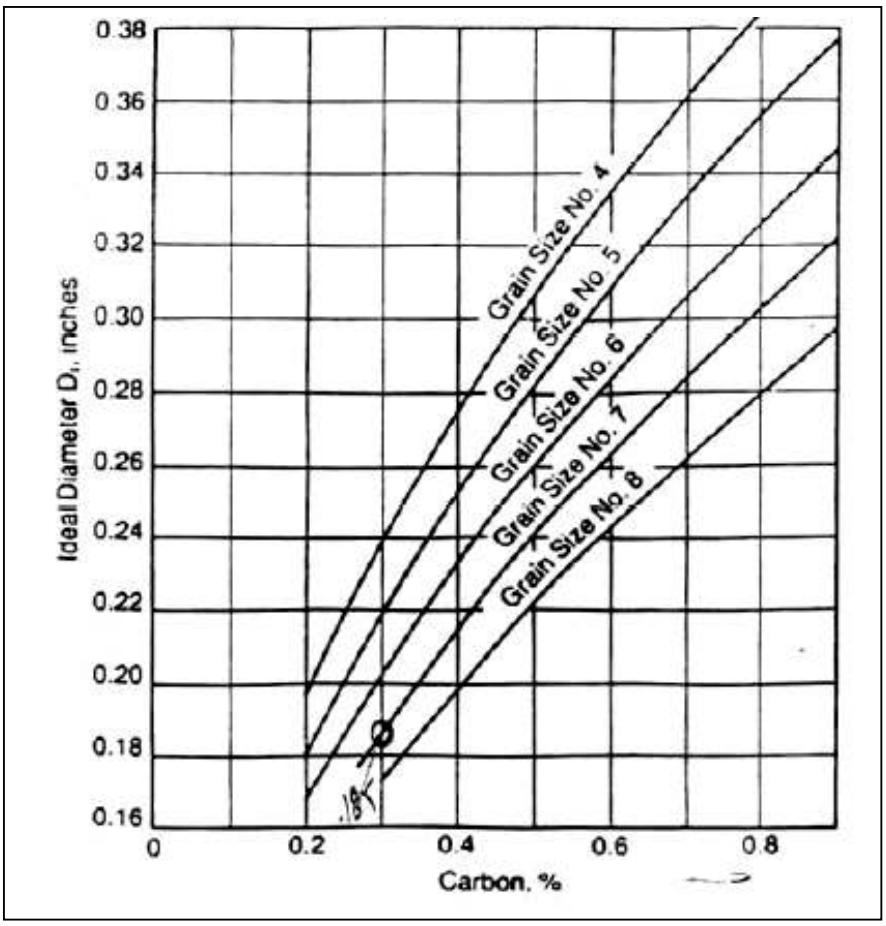

Fig. 5: Effect of ASTM grain size on hardenability of carbon steels (Courtesy ASTM).

The mechanical results versus tempering temperature shown in Table 8 and Fig.6, suggest possibly two temperatures where embrittlement is occurring. The first, at 250°C, is probably due to carbide film formation at grain boundaries and, in the case of the 1120°C material, at 350°C due to tramp element and/or oxygen segregation. On tempering at 400°C there is a recovery of toughness due to retained austenite transforming to bainite, which gives the highest impact value for the 1250°C material.

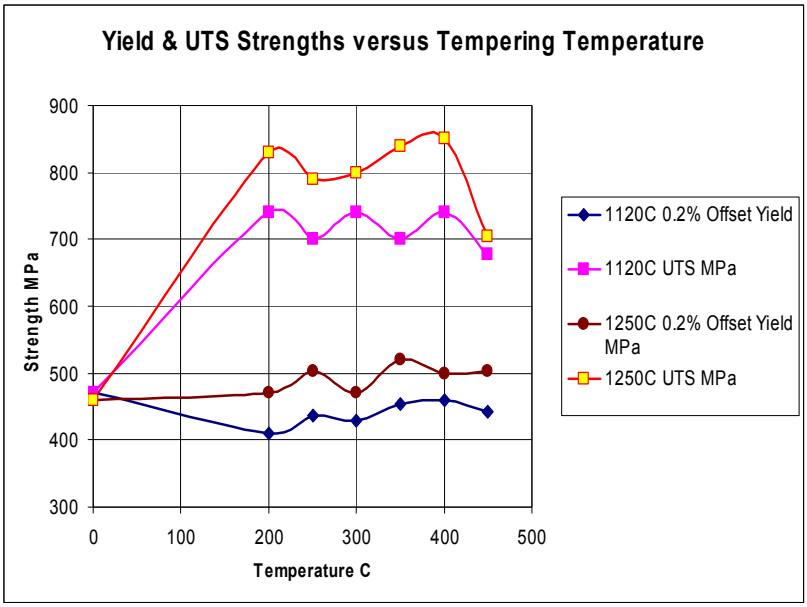

Fig. 6: Yield and Ultimate Tensile Strengths versus tempering temperature.

ACKNOWLEDGEMENTS
The authors acknowledge helpful discussions with and assistance of Prof. A.S Wronski of the University of Bradford in editing the MS and financial support of the Polish Research Committee under contract No.11.11.110.491.

REFERENCES

[1] A. Ciaś, S. C. Mitchell, A.S. Wronski, Proc. PM'98 World Congress on Powder Metallurgy, EPMA, Vol. 3, 1998, p.179.

[2] A. Ciaś, S. C. Mitchell, A. Watts, A.S. Wronski, *Powder Met*,**42**, 1999,. 227.

[3] S. C. Mitchell, A. S. Wronski, A. Ciaś: *Inżynieria Materiałowa*, **5**, 2001,. 633.

[4] A. Ciaś, M. Stoytchev, A. S. Wronski, Advances in Powder Metallurgy and Particulate Materials, MPIF, Vol.10, 2001, p. 131.

[5] A. Ciaś, M. Sułowski, S. C. Mitchell, A. S. Wronski, Proc. Euro PM 2001, Vol.4 , 2001, p. 246.

[6] S.C. Mitchell, A.S. Wronski, A. Ciaś, Advances in Powder Metallurgy and Particulate Materials MPIF, Vol. 2, 1999, p. 7.

[7] S. C. Mitchell, B. S. Becker, A. S. Wronski, Proc. 2000 PM World Congress, Kyoto, 2001, Vol. II, p. 923.

[8] A. Ciaś, S. C. Mitchell, K. Pilch, H. Ciaś, M. Sułowski and A. Wronski, *Powder Metallurgy*, **46**, 2003, p.165.

[9] A. Cias: Habilitation dissertation, Monograph No. 129, 2004, AGH Krakow.

[10] E. Dudrova, M.Kabátová, R. Bureš, R. Bidulský and A. S. Wronski, Proc. Int, Conf. ROPM 2005, Cluj-Napoca, 7-9 July 2005, p. 493.

[11] A. Salak, Ferrous Powder Metallurgy, Cambridge ISP, 1995, p.228.